Formation and growth of Bi-2223 phase in Bi-2223/Ag and Bi-2223/AgAu tapes

Xiaobo Ma[1], Shengnan Zhang[1],* , Jianqing Feng[1], Chengshan Li[1], Botao Shao[1], and Jianfeng Li[1]

[1] *Northwest Institute for Nonferrous Metal Research (NIN), Xi'an 710016, China*

ABSTRACT

Mono-filament Bi-2223/Ag and Bi-2223/AgAu tapes were fabricated by power-in tube technique. The Bi-2223 phase formation temperature and content of Bi-2223/Ag and Bi-2223/AgAu tapes were analyzed first. To have a quantitative understanding of growth process of Bi-2223 grains during the sintering process, the length and thickness of Bi-2223 platelets were measured. It is found that the growth rate in the length direction of Bi-2223 platelets was two orders of magnitude higher than that in the thickness direction and the Bi-2223 grains had same growth rate in the length direction for Bi-2223/Ag and Bi-2223/AgAu tape, but growth rate in the thickness direction was different. When sintering time reached 10 h, the average platelet thickness of Bi-2223/Ag and Bi-2223/AgAu tapes were 0.3 and 0.23 μm, respectively. This will bring about the difference in the phase content of Bi-2223, which is the key to affecting the current-carrying performance of the tape. The above results provided insightful information to understand both Bi-2223 phase growth of Bi-2223/AgAu tape and to improve its current-carrying property.

1 Introduction

Among high temperature superconductors (HTS), Ag-sheathed $Bi_2Sr_2Ca_2Cu_3O_{10+\delta}$ (Bi-2223) composite conductor is currently the primary HTS conductor available in lengths suitable for practical applications [1–4]. Many groups have investigated Ag and Ag alloy (including elements Mg, Au, Mn, Cu, Ni and Ti) as the sheath materials for fabrication Bi-2223 tape suitable for application such as power cable [5], motors [6, 7], magnets [8–11], as well as current lead [12–14]. The addition of Au into Ag sheath can

reduce the thermal conductivity of Bi-2223 tapes effectively [15], so Bi-2223/AgAu tape is a good choice for the fabrication of HTS current lead. However, several problems still remain in Bi-2223/AgAu superconducting tapes. The most important one is the lower Bi-2223 formation rate due to the low oxygen diffusion rate of AgAu sheath comparing with Ag sheath [16]. Considering that the phase evolution process of Bi-2223 involved with complex reactions and oxygen release/absorption process, the smaller oxygen diffusion rate could lead to slower change of local oxygen partial pressure of

superconducting cores, thus influenced the formation of Bi-2223 phase and critical current density. Due to the higher manufacturing costs and lower transport properties compared to Bi-2223/Ag tape, the applications of Bi-2223/AgAu tape are limited, so it is very necessary to improve critical current of Bi-2223/AgAu tapes.

During the PIT process, there are many parameters which can affect critical current of Bi-2223 tapes. First, the fabrication techniques for precursor powder, including solid state sintering [17], high energy milling [18], co-precipitation [19, 20], spray drying [21, 22] and spray pyrolysis [23], have been optimized. Meanwhile, the chemical composition of Bi-2223 precursor powders and chemical stoichiometry of Bi-2223 phase are important parameters [24–26]. Second, the influences of alloying additions on critical current and mechanical properties of Bi-2223 tapes have also been investigated [27–31]. Due to the change of mechanical properties and oxygen penetration rate of metal sheaths, the critical current varied greatly [32–34]. In these studies, however, the phase formation process and grain size which affect critical current of Bi-2223 tapes are not systematically evaluated. Therefore, it is quite necessary to study the phase evolution process in the AgAu sheathed tapes and to enhance their current capacity.

In the present study, the thermodynamic and kinetic differences of Bi-2223/Ag and Bi-2223/AgAu tapes during the heat treatment process were systematically investigated. Using step-by-step sintering + quenching method, the growth process of Bi-2223 platelet during the sintering of Bi-2223 tapes were analyzed, to reveal the difference in the phase formation process between Bi-2223/Ag and Bi-2223/AgAu tapes. This research will assist determining proper heat treatment of Bi-2223/AgAu tapes o improve its critical current that can be the focus of future application.

2 Experiment

Precursor powders with the nominal composition of $Bi_{1.76}Pb_{0.34}Sr_{1.93}Ca_{2.02}Cu_{3.06}O_x$ were prepared through a two-powder co-precipitation process with the initial phase assemblage of the (Bi, Pb)-2212, Ca_2CuO_3, and CuO [35]. The precursor powders were packed into pure Ag and AgAu5 wt% tubes ((outer diameter: φ12 mm, wall thickness: 1 mm). With a

series of swaging and drawing processes, single filament wires with diameter φ1.86 mm were obtained. The rolling processes for the two wires are identical, with the reduction rate of $\sim$ 20% per pass. Samples of as-rolled tapes with the length of 15 cm were sintered at 826 °C for different time under flowing Ar-7.5% O_2, and then quenched in air.

X-ray diffraction was done by an X-ray diffractometer (Bruker D8 Advance) with Cu-Kα radiation. The phase composition of core at Ag/superconductor interface, 0.11 mm distant from Ag/superconductor interface, and 0.16 mm distant from Ag/superconductor interface were characterized by X-ray diffraction after sheath was removed. The volume fractions of Bi-2223 and Bi-2212 phase can be calculated from the intensity I of some selected peaks by the following relation:

$$V_{2223}(\%) = I_{2223(0010)}/\left[I_{2223(0010)} + I_{2212(008)}\right] \times 100\% \tag{1}$$

$$V_{2212}(\%) = I_{2212(008)}/\left[I_{2223(0010)} + I_{2212(008)}\right] \times 100\% \tag{2}$$

where, $I_{2223\ (0010)}$ and $I_{2212\ (008)}$ are the intensities of (0010) peak of Bi-2223 and (008) peak of Bi-2212, respectively. The microstructure and composition were examined using JEOL 6700F scanning electron microscope equipped with Inca-X-Stream energy dispersive X-ray spectroscopy (EDX).

3 Results and discussion

Figure 1 shows DSC curves of mono-filamentary Bi-2223/Ag and Bi-2223/AgAu tapes. It can be seen from Fig. 1 that the positions of the characteristic peaks and the shape of the curves are basically the same as the temperature increases for different tapes. The 830–870 °C part is shown in the inset of Fig. 1, and the characteristic peak temperature is marked with an arrow. It can be seen that the formation temperature of Bi-2223 phase in Bi-2223/Ag and Bi-2223/AgAu tapes are 823 and 825 °C, and the melting decomposition temperature are 860 and 862 °C.

XRD patterns and Bi-2223 content at different regions along the thickness direction of Bi-2223/Ag and Bi-2223/AgAu tapes sintered at 826 °C for 15 h is shown in Fig. 2. Since Ag sheath can reduce the formation temperature of Bi-2223 phase, Bi-2223 phase content at the core surface is 83.9% and this value
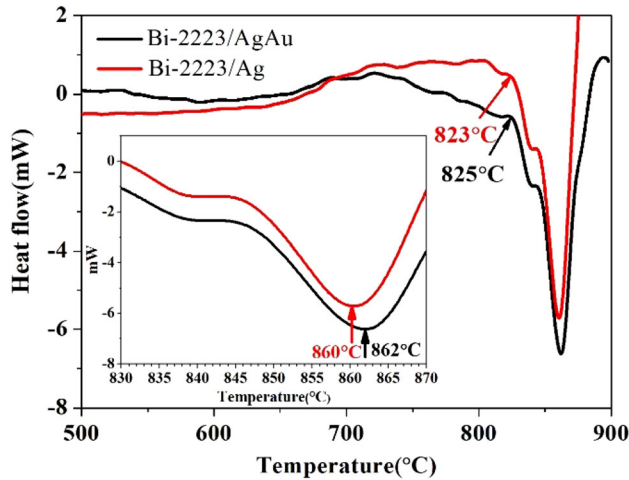
Fig. 1 DSC curves of mono-filamentary Bi-2223/Ag and Bi-2223/AgAu tapes

steadily decreased as the polished surface reached to the center of the core. The Bi-2223 phase contents are 77.8% and 75.9% at the regions which are 0.11 mm and 0.16 mm distant from core surface, respectively. However, Bi-2223 phase contents of Bi-2223/AgAu tape in same regions are always lower than that of Bi-

2223/Ag tape. The difference is the largest on core surface, which will gradually decrease when the region is closer to core. This is because oxygen diffusion rate in Ag sheath is larger than that in Ag alloy sheath (for example AgAu sheath) [16]. The difference of oxygen diffusion rate will influence oxygen partial pressure, which will lead to the change of Bi-2223 phase formation temperature and phase formation rate.

The backscattered electron images of Bi-2223/AgAu tapes sintered at 826 °C for different time have been shown in Fig. 3a–d. EDX results of different phases of sample d are shown in Fig. 3e. Combining EDX results and research results of Chen X P [36], the light gray phase is Bi-2212, the dark gray phase is Bi-2223, the white area is the amorphous phase formed by the liquid phase after quenching. When holding time reaches 3 h, only a small amount of long tape-shaped Bi-2223 platelets are randomly distributed in the superconducting core. As the holding time increases, the number of Bi-2223 platelets increase significantly. In addition, the length and thickness of some Bi-2223 platelets also increase, and the grain

Fig. 2 XRD patterns at different positions along the thickness direction of **a** Bi-2223/Ag tape; **b** Bi-2223/AgAu tape; **c** Bi-2223 phase content at different positions of Bi-2223/Ag and Bi-2223/AgAu tapes sintered at 826 °C for 15 h
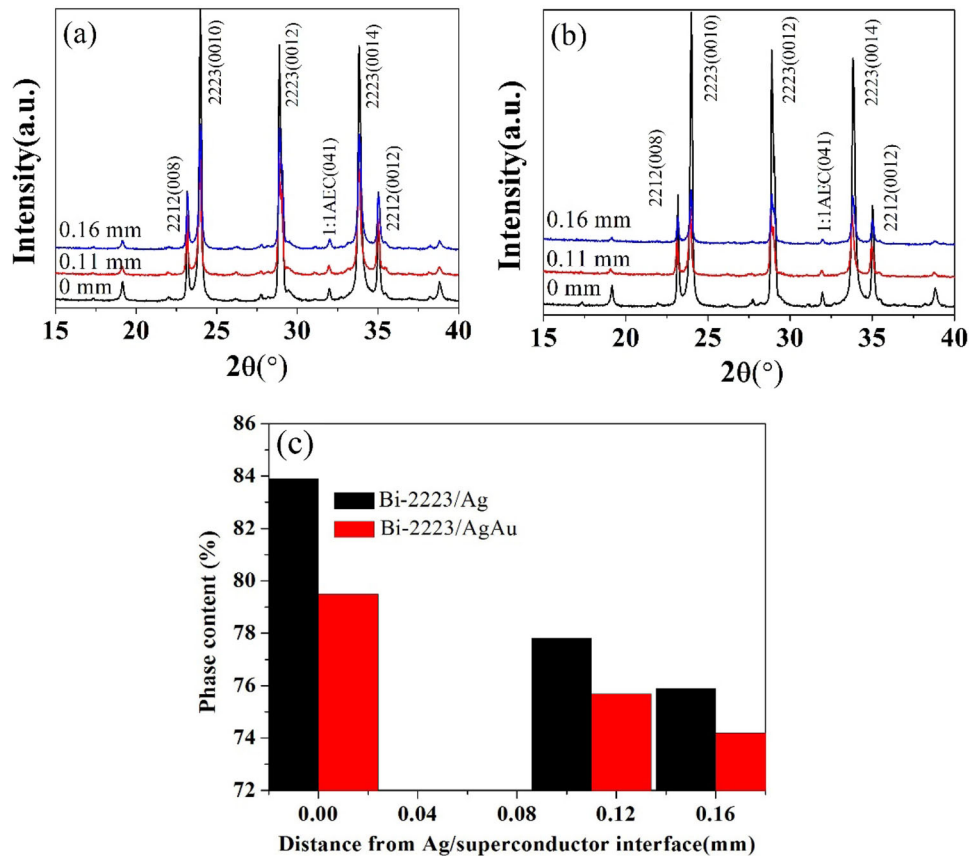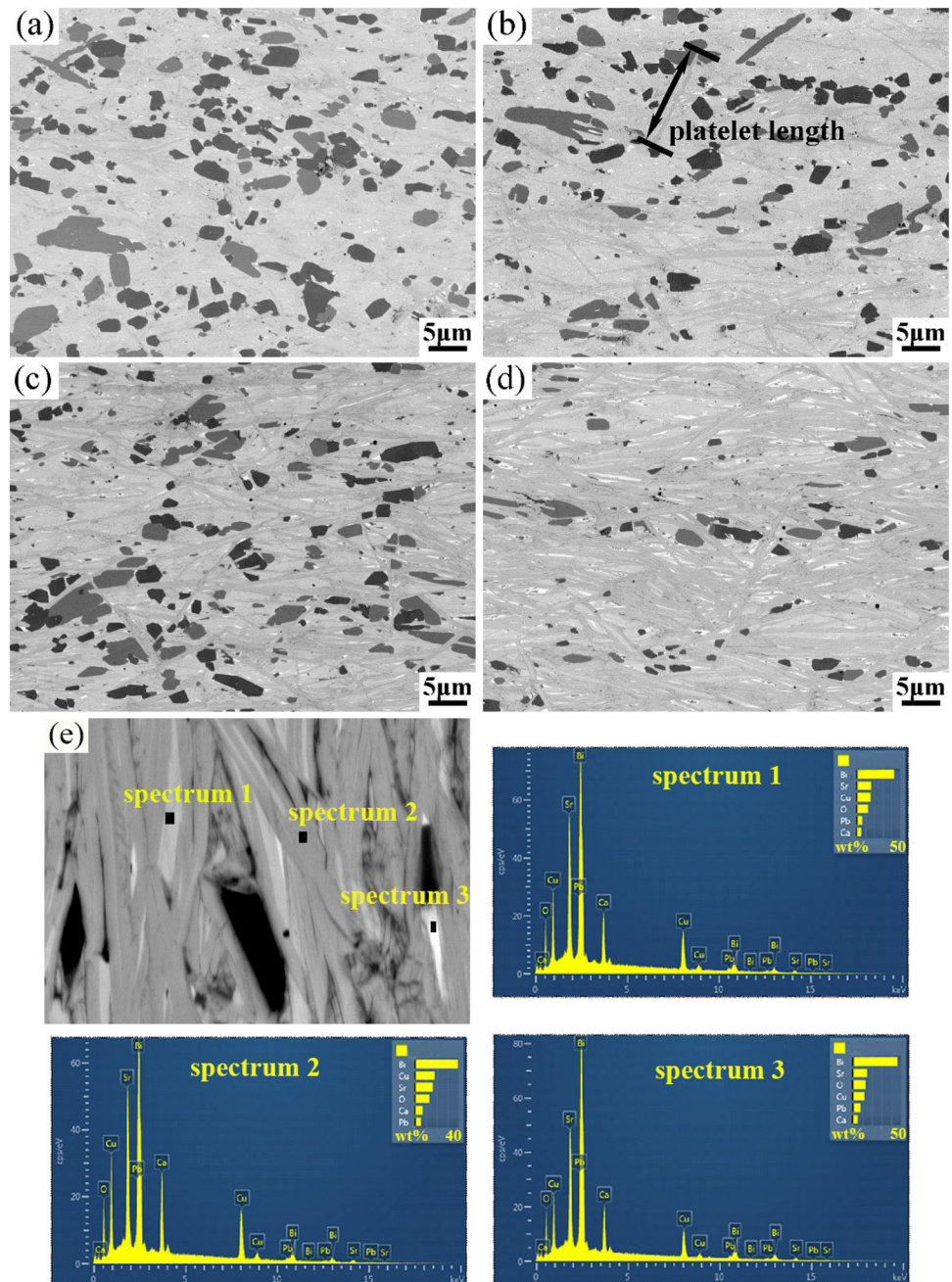
Fig. 3 SEM images of mono-filament Bi-2223/AgAu tapes sintered at 826 °C for different time **a** 3 h, **b** 5 h, **c** 10 h, **d** 15 h and **e** EDS results of different phases of sample **d**

arrangement of Bi-2223 platelets gradually tends to be the same, showing a certain degree of texture.

In order to have a quantitative understanding of the growth process of Bi-2223 platelets during the sintering process, the length of Bi-2223 platelets is measured by the image analysis software ImageJ®. For example, the length of Bi-2223 platelets is measured in Fig. 3b. Due to the serious overlap between Bi-2223 platelets after the holding time increases to 15 h, it is difficult to accurately measure the length of

Bi-2223 platelets. Therefore, the length of the Bi-2223 platelet in the tapes with the holding time of 3–10 h are only analyzed. Statistical distributions of Bi-2223 platelet length of Bi-2223/AgAu tape sintered at 826 °C for different time are shown in Fig. 4. According to the statistical results, the average Bi-2223 platelet length can be obtained by calculating the expected value of all the measured data. The results show that the average Bi-2223 platelet length increases from 5.9 μm of the tape sintered for 3 h to

12.9 μm of the tape sintered for 10 h. When holding time is less than 10 h, Bi-2223 platelet length increases very rapidly. Curves of average Bi-2223 platelet length and growth rate are shown in Fig. 5. During holding time increase from 3 to 10 h, Bi-2223 platelet length is continuously increasing, but the growth rate is continuously decreasing. Growth rate of the length decreases from 2.0 μm/h of the tape sintered for 3 h to 1.3 μm/h of the tape sintered for 10 h. This is because with the increase of Bi-2223 content and the decrease of liquid phase, there are more and more obstacles in the length direction, making it difficult to grow.

It can be seen from the inset in Fig. 4c, Bi-2223 platelet length distribution of Bi-2223/Ag and Bi-2223/AgAu tape is basically the same after sintering for 10 h. The average platelet length of mono-filamentary Bi-2223/Ag tape is 12.9 μm, while that of Bi-2223/AgAu tape is 12.8 μm. It indicates that for Bi-2223 tapes, the type of sheath has little effect on the growth rate in the length direction.

The backscattered electron images of Bi-2223/AgAu tapes sintered at 826 °C for different time are shown in Fig. 6. The thickness of Bi-2223 platelets with different holding time is measured by the image analysis software ImageJ®. For example, the
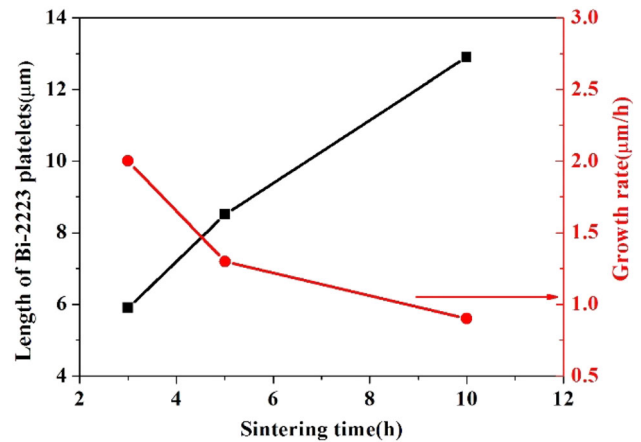

Fig. 5 Curves of average Bi-2223 platelet length and growth rate

thickness of Bi-2223 platelets is measured in Fig. 6c. Through the statistics of a large number of SEM photos, statistical distributions of Bi-2223 platelet thickness of mono-filamentary Bi-2223/AgAu tape sintered at 826 °C for different time are shown in Fig. 7. Due to the serious overlap between Bi-2223 platelets after the holding time increases to 50 h, it is difficult to accurately measure the thickness of Bi-2223 platelets. Therefore, the Bi-2223 platelet thickness in the tapes with the holding time of 3–20 h is only analyzed. According to the statistical results, the

Fig. 4 Bi-2223 platelet length of mono-filamentary Bi-2223/AgAu tape sintered at 826 °C for different time **a** 3 h, **b** 5 h, and **c** 10 h. The inset in figure **c** shows statistical distribution of Bi-2223 platelet length of mono-filamentary Bi-2223/Ag tape
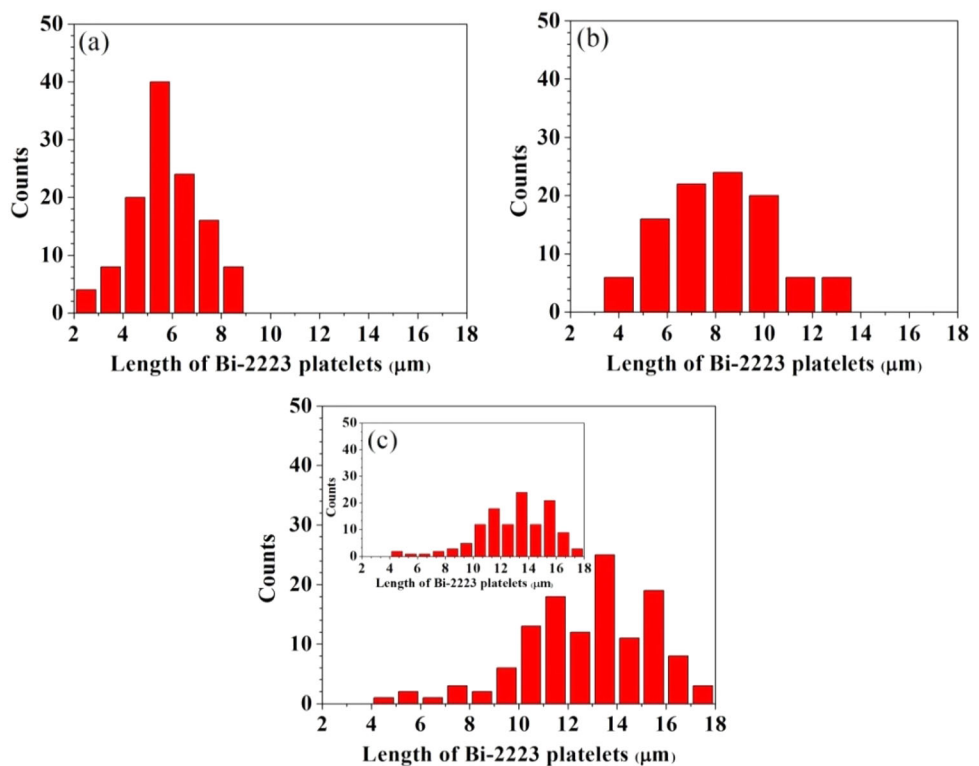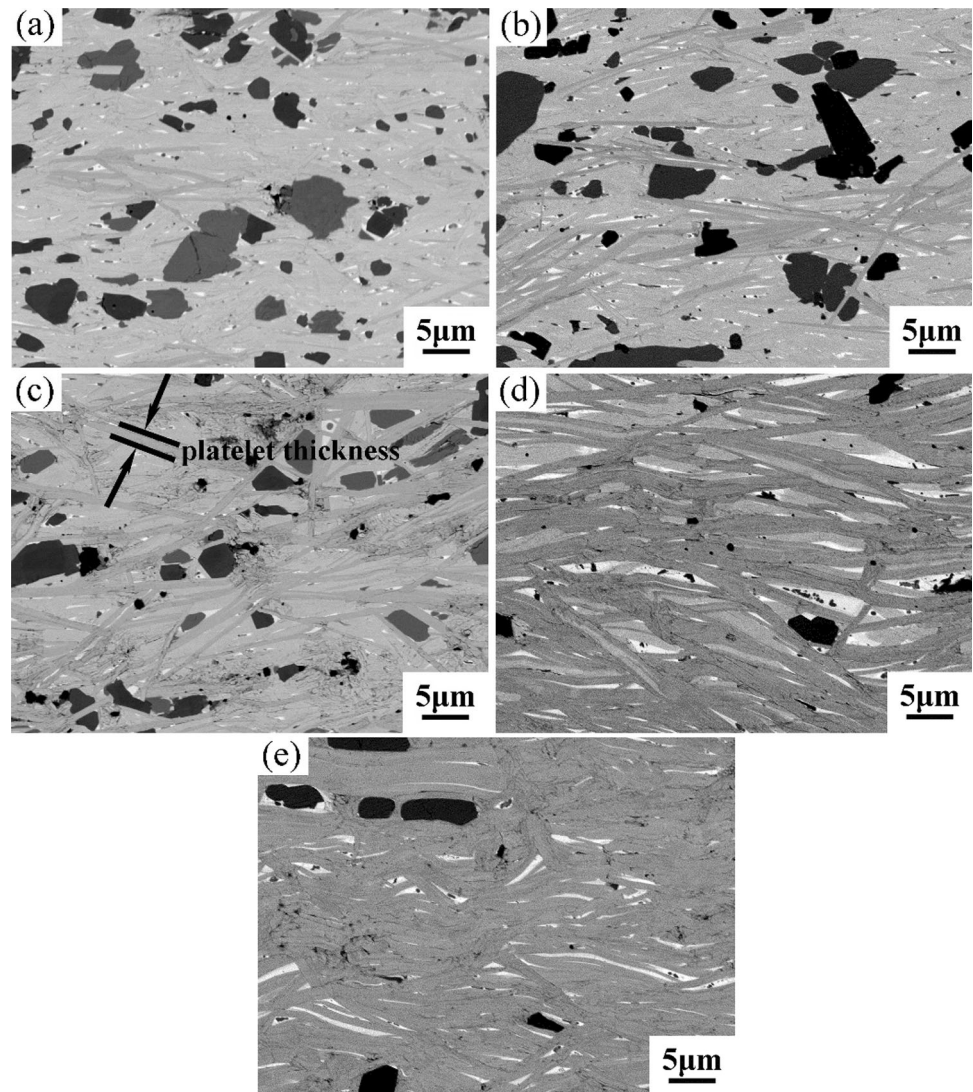
Fig. 6 SEM images of mono-filamentary Bi-2223/AgAu tapes sintered at 826 °C for different time **a** 3 h, **b** 5 h, **c** 10 h, **d** 20 h and **e** 50 h

average Bi-2223 platelet thickness can be obtained by calculating the expected value of all the measured data. The results show that the average Bi-2223 platelet thickness is 0.14, 0.17, 0.23 and 0.27 µm after holding for 3, 5, 10 and 20 h. The average thickness is 1–2 orders of magnitude smaller than the average length after the same holding time.

Curves of average Bi-2223 platelet thickness and growth rate are shown in Fig. 8. During holding time increase from 3 to 20 h, Bi-2223 platelet thickness is continuously increasing, but the growth rate of the thickness is continuously decreasing. Growth rate of the thickness decreases from 0.048 µm/h of the tape sintered for 3 h to 0.014 µm/h of the tape sintered for 20 h. The growth rate along the thickness direction is very slow compared to the growth rate along the length direction, which is two orders of magnitude lower than the growth rate along the length direction.

It can be seen from the inset in Fig. 7c, the number of platelet with larger thickness is more in Bi-2223/Ag tape compared with Bi-2223/AgAu tape, and the average platelet thickness of Bi-2223/Ag and Bi-2223/AgAu tapes are 0.3 and 0.23 µm, respectively. This is due to the low oxygen diffusion rate in AgAu sheath, and Bi-2223 grains grow very slowly along the thickness direction. The above results show that the difference in thickness brings about the difference in the content of Bi-2223, which is the key to affecting the current-carrying performance of the tape.

Based on the above analysis, the growth process of Bi-2223 grains in Bi-2223/AgAu tapes can be described as follows: as shown in Fig. 9, at the initial stage of the reaction, Bi-2223 grains nucleated at favorable

Fig. 7 Bi-2223 platelet thickness of mono-filamentary Bi-2223/AgAu tape sintered at 826 °C for different time **a** 3 h, **b** 5 h, **c** 10 h and **d** 20 h. The inset in figure **c** shows distribution of Bi-2223 platelet thickness of mono-filamentary Bi-2223/Ag tape
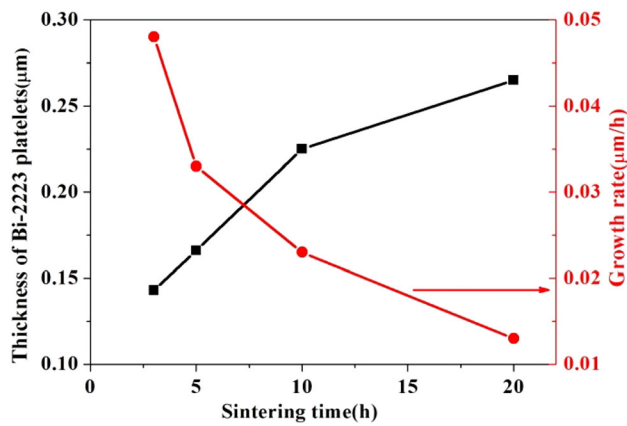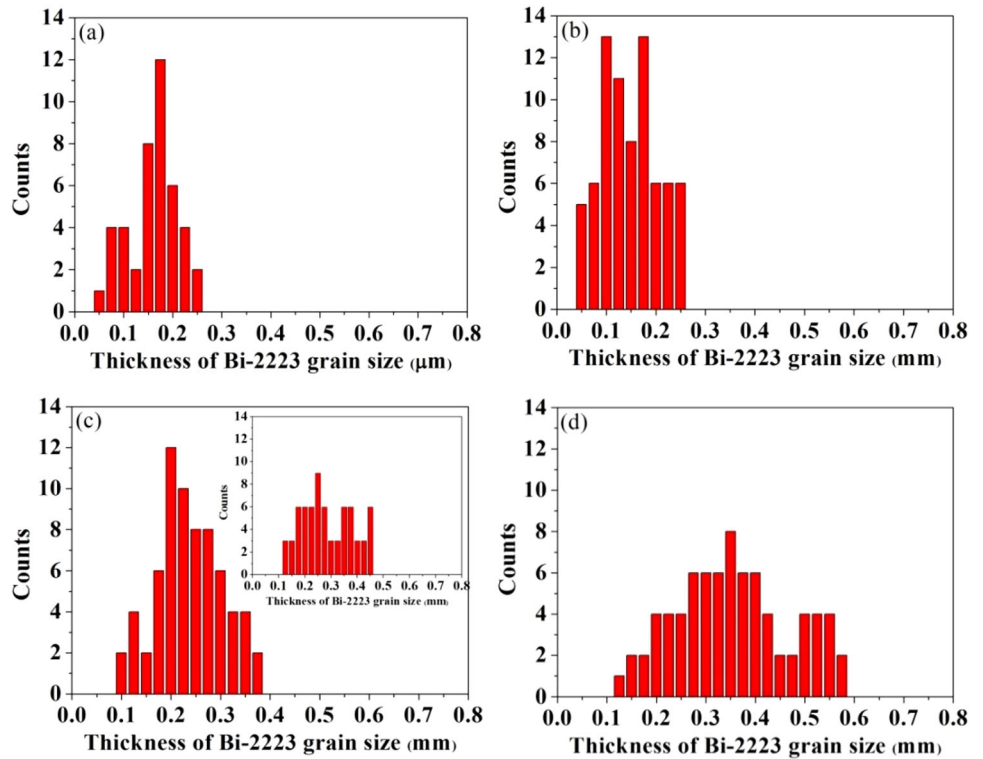

Fig. 8 Curves of average Bi-2223 platelet thickness and growth rate

positions in the core. With the increasing of holding time, the nucleated grains at the early stage begin to grow. At this time, the grains grow both along the length direction and the thickness direction, and the growth rate along length direction is faster. After the sintering time reaches 20 h, Bi-2223 platelets overlap in the length direction. so it is difficult to continue to grow along the length direction, the Bi-2223 grains only grow along the thickness direction.

4 Conclusion

In this study, Bi-2223 phase formation temperature, Bi-2223 phase content and growth differences in the length and thickness direction of Bi-2223 platelet of Bi-2223/Ag and Bi-2223/AgAu tape are systematically investigated by SEM and DSC. First, The formation temperature of Bi-2223 phase in Bi-2223 / AgAu tape is 2 °C higher than that of Bi-2223 /Ag tape. The change of formation temperature of Bi-2223 phase will decrease Bi-2223 content. Meanwhile compared with the traditional Bi-2223/Ag tape, Bi-2223 grains in the Bi-2223/AgAu tape have the same growth rate along the length direction of Bi-2223 platelet. But the growth rate along the thickness direction is slower. Under the same heat treatment conditions, the Bi-2223 content and grain size of the Bi-2223/AgAu tape is lower and smaller, so current density is lower than Bi-2223/Ag tape. The heat treatment process of Bi-2223/AgAu tape needs to be optimized in order to obtain higher current density. The results of this study provided a new opportunity for the further enhancement of the current carrying capacity of Bi-2223/AgAu tapes for practical application. Though lots of important results are obtained, how the oxygen partial pressure inside

Fig. 9 Schematic diagram of Bi-2223 grain growth process
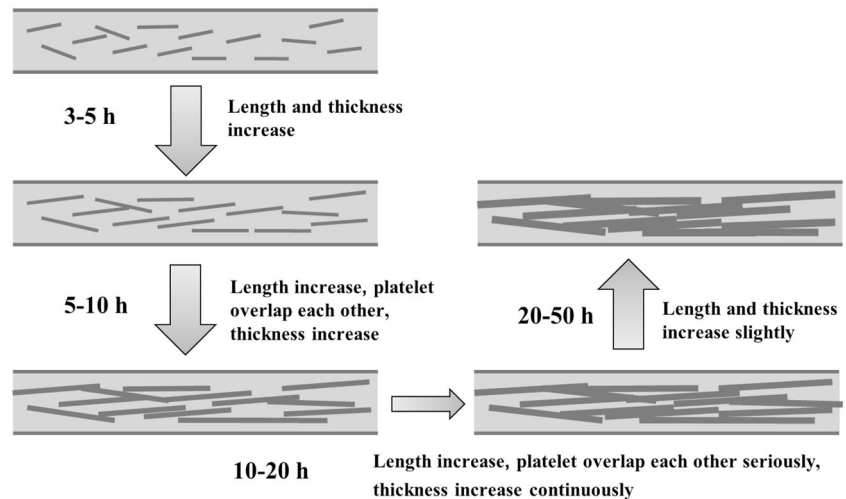
superconductor filaments varied in different sheathed Bi-2223 tapes still call for more detail investigation. What is the proper oxygen partial pressure for different sheaths and precursor powder still need to be found urgent in the future.

Acknowledgements

Author contributions

All authors contributed to the study conception and design. SZ and CL contributed to the conception of the study, XM and BS performed the experiment; XM and SZ performed the data analyses and wrote the manuscript; JF and JL helped perform the analysis with constructive discussions.

Data availability

The datasets generated during and/or analyzed during the current study are available from the corresponding author on reasonable request.

Declarations

Conflict of interest All authors certify that they have no affiliations with or involvement in any organization or entity with any financial interest or non-financial interest in the subject matter or materials discussed in this manuscript.

Research involving human and animals participants This research does not involve any human and animals participants.

References

1. M. Nassi, HTS prototype for power transmission cables: recent results and future programmes. Supercond. Sci. Technol. **13**(5), 460 (2000)

2. K. Sato, T. Kato, K. Ohkura, S. Kobayashi, K. Hayashi, Performance of all high-Tc superconducting magnets generating 4 T and 7 T at 20 K. Supercond. Sci. Technol. **13**(1), 18 (2000)

3. K. Hayashi, S. Hahakura, N. Saga et al., Development of Ag-sheathed Bi2223 superconducting wires and their application to magnets. IEEE Trans. Appl. Supercond. **11**, 3281–3284 (2001)

4. Y. Zhang, C.C. Koch, J. Schwartz et al., Synthesis of $Bi_2Sr_2CaCu_2Ox$ superconductors via direct oxidation of metallic precursors. Supercond. Sci. Technol. **27**, 055016 (2014)

5. M. Ohya, Y. Inagaki, K. Tatamidani et al., Japan's first live power transmission using 3-in-one superconducting cable (high-temperature superconducting cable demonstration project). SEI Tech. Rev. **76**, 45–54 (2013)

6. A. Gonzalez-Parada, F.J. Espinosa-Loza, A. Castaneda-Miranda et al., Application of HTS BSCCO tapes in an ironless axial flux superconductor motor. IEEE Trans. Appl. Supercond. **22**, 5201004 (2012)

7. B. Liu, R. Badcock, H. Shu, L. Tan, J. Fang, Electromagnetic characteristic analysis and optimization design of a novel

HTS coreless induction motor for high-speed operation. IEEE Trans. Appl. Supercond. **28**, 5202405 (2018)

8. S. Hanai, T. Tsuchihashi, S. Ioka et al., Development of an 11 T BSCCO insert coil for a 25 T cryogen-free superconducting magnet. IEEE Trans. Appl. Supercond. **27**, 4602406 (2017)

9. W.S. Marshall, M.D. Bird, A. Godeke, Bi-2223 test coils for high-resolution NMR magnets. IEEE Trans. Appl. Supercond. **27**, 4300905 (2017)

10. Y. Yanagisawa et al., Combination of high hoop stress tolerance and a small screening current-induced field for an advanced Bi-2223 conductor coil at 4.2 K in an external field. Supercond. Sci. Technol. **28**, 125005 (2015)

11. S. Iguchi, Y. Yanagisawa, M. Takahashi et al., Shimming for the 1020MHz LTS/Bi-2223NMR magnet. IEEE Trans. Appl. Supercond. **26**, 4303507 (2016)

12. C. Liu, K. Ding, T. Zhou et al., Development on 6 kA HTS current leads. Cryogenics **5**, 18–22 (2015)

13. T. Zhou, K. Lu, K. Ding et al., Design and development of 16-kA HTS current lead for HMFL 45-Tmagnet. IEEE Trans. Appl. Supercond. **25**, 4802906 (2015)

14. T. Tsurudome, J. Yoshida, H. Ookubo et al., Reliability of Bi-2223/AgAu current leads for Cryocooled Superconducting-magnet. IEEE Trans. Appl. Supercond. **23**, 4802204 (2013)

15. T. Naito, H. Fujishiro, Y. Yamada, Thermal conductivity of single and multi-stacked DI-BSCCO tapes. Cryogenics **49**, 429–432 (2009)

16. M. Quilitz, W. Goldacker, Oxygen exchange in Bi(2223) tapes with Ag and alloyed AgMg sheaths monitored by a thermogravimetrical relaxation method. Supercond. Sci. Technol. **11**(3), 577–583 (1998)

17. M. Zouaoui, A. Ghattas, M. Annabi et al., Effect of nano-size ZrO2 addition on the flux pinning properties of (Bi, Pb)-2223 superconductor. Supercond. Sci. Technol. **21**, 125005 (2008)

18. N. Darsono, A. Imaduddin, K. Raju, D.H. Yoon, Synthesis and characterization of $Bi_{1.6}Pb_{0.4}Sr_2Ca_2Cu_3O_7$ superconducting oxide by high-energy milling. J. Supercond. Nov. Magn. **28**(8), 2259–2266 (2015)

19. C.B. Mao, L. Zhou, X.Y. Sun et al., Co-precipitation-based micro-reactor process to synthesize soft-agglomerated ultra-fine BiPbSrCaCuO powder with low carbon content. Physica C. **281**, 35–44 (1997)

20. D.H. Chen, C.Y. Shei, S.R. Sheen et al., Preparation of superconducting Bi-Pb-Sr-Ca-Cu-O Compounds by Oxalate Co-precipitation. Jpn. J. Appl. Phys. **30**(6R), 1198–1203 (1991)

21. R. Bao, X.H. Song, S.S. Chen et al., The influences of powder processing variables on the properties of Bi-2223/Ag tapes. IEEE Trans. Appl. Supercond. **23**(3), 6400704 (2013)

22. X.D. Su, J.M. Yoo, J.W. Ko et al., The influence of precursor powders on the phase evolution, grain size and transport current properties of BSCCO 2223 Ag-sheathed tapes. Physica C. **331**, 285–291 (2000)

23. B.A. Marinkovic, P.M. Jardim, F. Rizzo et al., Characterization and phase transitions of $(Bi, Pb)2Sr2Ca2Cu3Ox$–Ag composite powder obtained by spray pyrolysis. Mater. Chem. Phys. **94**, 233–240 (2005)

24. K. Osamura, S. Nonaka, M. Matsui, Non superconducting phases and their influence on critical current density in Ag/Bi2223 tapes. Physica C. **257**, 79–85 (1996)

25. X. Ma et al., Influences of Pb content on the critical current of Bi-2223 multi-filamentary tapes. Mater. Lett. **162**, 5–8 (2016)

26. P. Majewski, B. Hettich, K. Schulze, The phase equilibria of $Bi_2Sr_2Ca_2Cu_3O_{10}$ in the system Bi_2O_3–SrO–CaO–CuO. Physica C. **185–189**, 469–470 (1991)

27. M.Y. Li, C.L. Ye, J. Liu, Microstructure and properties of Bi-2223/Ag/Ni tapes. Rare Met. **31**, 556–559 (2012)

28. H.P. Yi, X.H. Song, L. Liu et al., Effect of alloying additions to Ag on thermal conductivity, electrical and mechanical properties of Ag-sheathed Bi-2223 tapes. Physica C. **426–431**, 1176–1180 (2005)

29. X.P. Chen, X.W. Yu, M. Liu et al., Fabrication and properties of Ag-Ni bimetallic sheathed (Bi, Pb)-2223 tapes. J. Supercond. Novel Magnetism. **25**, 1501–1507 (2012)

30. J-C. Grivel, Composite metallic sheathes: The key to low-cost, high strength $(Bi, Pb)_2Sr_2Ca_2Cu_3O_{10}$-based tapes, Supercond. Sci. Technol. 20, 1059–1064 (2007).

31. R.P. Aloysius, A. Sobha, P. Guruswamy, U. Syamaprasad et al., Bend strain and tensile stress characteristics of (Bi, Pb)-2223/Ag-Cu alloy sheathed tapes. Supercond. Sci. Technol. **14**, 85–89 (2001)

32. X.P. Chen, X.W. Yu, R. Xiao et al., Critical current enhancement in Bi-2223/Ag superconducting tapes by controlling its first sintering process. J. Alloys Compounds. **509**, 1090–1093 (2010)

33. T.M. Qu, Z. Han, R. Flukiger, Phase evolution during post-annealing and its influence on critical currents of (Bi, Pb)-2223/Ag tapes. Physica C **444**, 71–76 (2006)

34. T.M. Qu, L. Zhao, X.C. Wang et al., The influence of post-annealing on the $Pb_3(Bi_{0.5}Sr_{2.5})Ca_2CuO_y$ phase evolution and superconducting properties of (Bi, Pb)-2223/Ag tapes. Physica C **463–465**, 833–836 (2007)

35. Y. Nakamura, R. Inada, Phase formation mechanism and properties of Ag-sheathed (Bi, Pb)-2223 tapes prepared by two-powder method. Physica C. **392–396**, 1015–1019 (2003)

36. X.P. Chen, Z. Han, M.Y. Li et al., Observation of the formation and growth of secondary phase in Bi-2223/Ag tapes. Physica C. **391**, 363 (2003)